

**Formation of novel ene-yne substituted β -diketonato
ruthenium(III) complexes by the Heck-like reactions on
coordinated ligand†**

Yoshimasa Hoshino^{a,*}, Fumika Ozaki^a, Satoshi Igarashi^b, and Yasuhiko Yukawa^c

^aDepartment of Science and Information Communication Technology, Graduate School of Education, Nagasaki University, 1-14 Bunkyo-machi, Nagasaki 852-8521, Japan.

^bDepartment of Chemistry, Faculty of Education, Niigata University, 8050 Ikarashi Nino-cho, Niigata 950-2181, Japan.

^cDepartment of Environmental Science, Faculty of Science, Niigata University, 8050 Ikarashi Nino-cho, Niigata 950-2181, Japan.

Submitted to *Inorganica Chimica Acta*

†Dedicated to Professor Wolfgang Kaim on the occasion of his 60th birthday

*Corresponding author. Tel & Fax: +81 (0)95 819 2332.

E-mail address: hoshino@nagasaki-u.ac.jp (Y. Hoshino)

Abstract

Two new ene-yne substituted 2,4-pentanedionatoruthenium(III) complexes formed by the Heck-like reactions in the course of the Sonogashira reactions. The two complexes are structural isomers; one is $[\text{Ru}(E-1,4\text{-mBSima})(\text{dpm})_2]$ and another is $[\text{Ru}(E-2,4\text{-mBSima})(\text{dpm})_2]$, where *E*-1,4-mBSima is *E*-3-(1,4-bis(trimethylsilyl)-1-butene-3-ynyl)-2,4-pentanedionate, *E*-2,4-mBSima is *E*-3-(2,4-bis(trimethylsilyl)-1-butene-3-ynyl)-2,4-pentanedionate, and dpm is dipivaloylmethanate (2,2,6,6-tetramethylheptan-3,5-dionate). Both of complexes have been characterized by ^1H NMR and infrared spectroscopies, mass spectrometry, and electrochemistry. $[\text{Ru}(E-1,4\text{-mBSima})(\text{dpm})_2]$ has also been characterized by X-ray crystallography. The ruthenium(III) is coordinated in an octahedral arrangement by the oxygen atoms of three β -diketonate ligands. The dihedral angle between the 2,4-pentanedionato chelate ring and the ene-yne plane on the *E*-1,4-mBSima ligand is 91° . The ene-yne group in $[\text{Ru}(E-1,4\text{-mBSima})(\text{dpm})_2]$ is fixed either in the solution state suggested by the ^1H NMR spectrum with no symmetry.

Keywords: Ruthenium(III) complex, β -Diketone complex, Acetylenic compounds, X-Ray crystal structure, ^1H NMR spectroscopy, DFT calculations

1. Introduction

Organometallics and metal complexes with one or several terminal alkynes are valuable building blocks for preparation of bi-, oligo-, or polynuclear complexes used to probe electronic and/or magnetic metal-metal interactions [1]. We have demonstrated that ruthenium complexes with terminal alkynes on β -diketonato chelates are useful starting materials for preparation of bi-, oligo-, and polynuclear complexes exhibiting characteristic electronic communications[2]. However, a precursor of the desired starting complex with an ethynyl group for binuclear complexes, ((3-trimethylsilyl)ethynyl-2,4-pentanedionato)ruthenium(III) complex (**1**) is only obtained up to ca. 40% yield, through the reaction of (3-iodo-2,4-pentanedionato)ruthenium(III) complex (**2**) with trimethylsilylacetylene in the Sonogashira cross-coupling reaction as shown in scheme 1[2a]. In the case of a precursor of a ruthenium complex with three ethynyl groups for the polymer, the yield is at most a few percent[2f]. The low yield often prevents progress of study on molecular bridge composed of acetylenic links and β -diketonato chelate, propagating electrons and/or spins. In general organic compounds with terminal alkynes can be obtained in good yield (ca. 60 - 90%) from the corresponding halide compounds [3]. Recently Bonvoisin et al. have shown that a protected ethynyl group can be introduced into a γ -position of a (β -diketonato)bis(bipyridine)ruthenium(II) complex with very good yield (62%) using a (3-bromo-2,4-pentanedionato)ruthenium complex and (triisopropylsilyl)acetylene under microwave irradiation[4]. They pointed out only one spot on thin-layer chromatography (TLC) plate of the reactant mixture after irradiation. On the other hand, in the course of preparing complex **1**, we always detected two unidentified ruthenium species on TLC plate at any reaction conditions. It is, therefore, important to

identify these unidentified ruthenium species and to elucidate mechanism of the formation reaction in order to find reaction conditions in the better yield of **1**.

We report here identification of the two unidentified ruthenium complexes, new ene-yne substituted ruthenium(III) species, [Ru(*E*-1,4-mBSima)(dpm)₂] (**3**) and [Ru(*E*-2,4-mBSima)(dpm)₂] (**4**), where *E*-1,4-mBSima is *E*-3-(1,4-bis(trimethylsilyl)-1-butene-3-ynyl)-2,4-pentanedionate, *E*-2,4-mBSima is *E*-3-(2,4-bis(trimethylsilyl)-1-butene-3-ynyl)-2,4-pentanedionato, and dpm is dipivaloylmethanate (2,2,6,6-tetramethylheptan-3,5-dionate), as well as the mechanism of the formation reaction. Both species have been characterized by IR, ¹H-NMR spectra and mass spectroscopy. Structure of one species has been determined by single-crystal X-ray structure analysis and characterized by DFT calculations.

[Scheme 1]

2. Experimental

2.1 General Information

Elemental analyses were carried out on a Yanaco MT-2 and a Perkin Elmer 2400 II. ¹H NMR spectra were recorded with a JEOL JNM GX-400 spectrometer in C₆D₆. Chemical shifts are reported in δ units using TMS in C₆D₆ as an external reference. Mass spectra were recorded with a JEOL JMS-DX303 instrument. The infrared (IR) absorption spectra were recorded on a JASCO FT/IR-350 spectrophotometer using KBr pellet in 4000–400 cm⁻¹ region. Electrochemical measurements were made at +25°C with a HECS 311C

potentio-galvanostat, a Huso HECS 321B potential sweep unit, and a Riken Denshi model F-3DGX-Y recorder. Acetonitrile containing 0.1 mol dm^{-3} TBABF₄ was used as a base solution. The test electrode was a platinum disk electrode (1.6 mm diameter). The reference electrode used was Ag/AgCl in 3 mol dm^{-3} NaCl aq. Ferrocene was used as an internal reference. The potential of ferrocenium/ferrocene (Fc⁺/Fc) couple was 0.48 V, and the peak separation was 70 mV, which was independent of the sweep rate (20-100 mV s⁻¹).

Density functional theory (DFT) electronic structure calculations on [Ru(*E*-1,4-*mBSima*)(dpm)₂] (**3**) were carried out with the Gaussian 03 program[5] using the UB3PW91 functional[6] with D95* (C, O, and H) and LANL2DZ (Si and Ru) basis sets.

2.2 Reagents

Trimethylsilylacetylene (98%), dichlorobis(triphenylphosphine)palladium(II), deuterated benzene (C₆D₆, 99.6 atom % D), and tetrakis(triphenylphosphine)palladium(0) were purchased from Aldrich Chemical Co., Ltd., copper(I) iodide (99.5%) from Wako Chemicals. Triethylamine (Wako Chemicals) was dried over potassium hydroxide, and acetonitrile for electrochemical measurements (HPLC grade, Wako Chemicals) over 3 Å molecular sieves. All other commercially available reagents were used without further purification.

2.3 Synthesis of complexes

2.3.1 Synthesis of [Ru(*E*-1,4-*mBSima*)(dpm)₂] (**3**)

The synthetic procedure is basically the same as that of complex **1** [2a], however scale and isolation procedure are different from those of complex **1**.

First, 300 cm³ of triethylamine containing 2.2 g (3.4 mmol) of **2** [2a] and 0.82 g (8.3

mmol) of trimethylsilylacetylene were stirred under N₂ with PdCl₂(PPh₃)₂ or Pd(PPh₃)₄ (0.078 mmol) and 83 mg of CuI (0.74 mmol). The progress of the reaction was checked by TLC (silica gel / benzene(1)-hexane(1)) every other day. When the reaction ceased, 0.45 g of the acetylenic compound and the same amounts of catalysts were added to the mixture. This procedure was repeated four times (the total amount of substance of the acetylene, Pd complex, and CuI was 2.6 g (26.7 mmol), 0.27 g (0.39 mmol), and 0.41 g (3.8 mmol), respectively; then the reaction mixture was stirred for 19 days at room temperature. Two unidentified ruthenium species were detected on a TLC plate of a reactant mixture (silica gel / benzene(1)-hexane(1)); complex **1** exhibited an *R_f* value of 0.49, the other two complexes had *R_f* values of 0.43 (complex **3**) and 0.41 (complex **4**), respectively. The residue obtained after the removal of the solvent was extracted with a mixture of benzene-hexane (3:2 by volume). The extract was applied onto a column of Merck Silica gel 60 (230-400 mesh), and the column was developed with the mixture. The eluate of the second, red-brown band was collected. The residue after the removal of the solvent was dissolved in a mixture of hexane-ethyl acetate (30:1 by volume). The solution was subjected flush column chromatography (Merck silica gel 60 developed with the mixture of hexane-ethyl acetate). The eluate of the first, orange band was collected, and then the solvent was evaporated off; yield 0.25 g (0.33 mmol, 9.7 %) for [Ru(*E*-1,4-mBSima)(dpm)₂] (**3**) (*E*-1,4-mBSima⁻ = *E*-3-(1,4-bis(trimethylsilyl)-1-butene-3-ynyl)-2,4-pentanedionate) in crystals.

Complex **3** was dissolved in hot ethanol, and the solution was left to stand in the dark. After a week, red, plate crystals were obtained. Anal. calcd for C₃₇H₆₃O₆RuSi₂; C, 58.39; H, 8.34. Found C, 58.22; H, 8.19. MS (EI) *m/z* 761(M⁺), 468([Ru(dpm)₂]⁺). IR (KBr) 2155 cm⁻¹ (C≡C). ¹H NMR (C₆D₆) δ = 4.97 (s, 1H, C=CH); 3.28 (s, 9H, C(CH₃)₃); 2.96 (s, 9H, C(CH₃)₃); 2.01 (s, 9H, C(CH₃)₃); 1.34 (s, 3H, CH₃); 1.21 (s, 12H, CH₃ + C(CH₃)₃); 1.11 (s,

9H, Si(CH₃)₃); -0.79 (s, 9H, Si(CH₃)₃); -30.8 (s, 1H, CH); -54.2 (s, 1H, CH). mp 158 °C.

Formal potential $E^\circ((E_p^a + E_p^c) / 2) = 0.45$ V and ca. -1.43 V (vs. Fc⁺/Fc).

2.3.2 Synthesis of [Ru(*E*-2,4-*mBSima*)(dpm)₂] (**4**)

The procedure is the same as for the synthesis of [Ru(*E*-1,4-*mBSima*)(dpm)₂] (**3**) except for the eluate collected in the course of the second chromatography. The eluate of the second, red-brown band was collected, and then the solvent was evaporated off; yield 0.17 g (0.22 mmol, 6.5 %) for [Ru(*E*-2,4-*mBSima*)(dpm)₂] (**4**) (*E*-2,4-*mBSima*⁻ = *E*-3-(2,4-bis(trimethylsilyl)-1-butene-3-ynyl)-2,4-pentanedionate) in amorphous. Anal. calcd for C₃₇H₆₃O₆RuSi₂; C, 58.39; H, 8.34. Found C, 59.56; H, 9.99. MS (EI) *m/z* 761(M⁺), 468([Ru(dpm)₂]⁺), 293(ligand). IR (KBr) 2117 cm⁻¹ (C≡C). ¹H NMR (C₆D₆) δ = 44.6 (s, 1H, C=CH); 2.57 (s, 18H, C(CH₃)₃ X 2); 2.23 (s, 18H, C(CH₃)₃ X 2); 0.77 (s, 9H, Si(CH₃)₃); 0.64 (s, 6H, CH₃ X 2); 0.31 (s, 9H, Si(CH₃)₃); -42.4 (s, 2H, CH X 2). Formal potential $E^\circ((E_p^a + E_p^c) / 2) = 0.45$ V and $E_p^c = -1.56$ V (vs. Fc⁺/Fc).

2.4 X-ray crystallography of [Ru(*E*-1,4-*mBSima*)(dpm)₂] (**3**)

A red prismatic crystal for X-ray diffraction experiments was mounted on a glass fiber. Measurements were made on a Rigaku RAXIS-IV diffractometer to a maximum 2θ value of 55.1° for complex **3** with graphite-monochromated Mo Kα (λ = 0.7107 Å) radiation. The data were corrected for Lorentz and polarization effects. The structure was solved by a heavy atom method (TeXsan) [7]. Refinement of complex **3** was carried out on F^2 using full-matrix least-squares calculations, which minimized the function $\Sigma w(F_o^2 - F_c^2)^2$. A correction for secondary extinction (see Table 1) was applied. The non-hydrogen atoms were refined with

anisotropic thermal parameters. Hydrogen atoms were included but not refined. All the calculations for the structure determination were carried out on a TeXsan crystallographic software package [7].

3. Results and discussion

3.1 Structure Determinations of Complexes **3** and **4**

The EI mass spectra of both ruthenium complexes showed the same molecular ion peak and the same fragment peak at $m/z = 761$ and at 468 , respectively, indicating the same composition formula $C_{37}H_{63}O_6RuSi_2$ (FW = 761.14) and the same partial structure $[Ru(dpm)_2]^+$ (FW = 467.61). The IR spectrum exhibited a weak peak at 2155 cm^{-1} for **3** and at 2117 cm^{-1} for **4**, respectively, indicating the existence of a $C\equiv C$ group. The 1H NMR spectrum of **3** exhibited 10 peaks between 5 and -55 ppm, while complex **4** exhibited only 7 peaks. This indicates that **3** has no symmetry even in solution, while **4** has C_2 symmetry in solution. Both **3** and **4** exhibited a Nernstian one-electron oxidation step at 0.450 V (vs. Fc^+/Fc) and a quasi-Nernstian one-electron reduction step at ca. -1.43 V for **3** and -1.56 V (the cathodic peak potential) for **4** with subsequent reactions in 0.1 mol dm^{-3} TBABF₄-CH₃CN. The ratio of I_p^c/I_p^a at the oxidation step is unity, but the I_p^c is larger than the I_p^a at the reduction step, indicating the subsequent reactions. These results suggest that complex **4** is a structural isomer of complex **3**. Fortunately, red single crystals of **3** were obtained by recrystallizing from ethanol at ambient temperature.

Summary of the crystal data and structure refinements for complex **3** and selected bond lengths and angles as well as dihedral angle are given in Tables 1 and 2. Figure 1 shows the

ORTEP drawing of complex **3** and the numbering scheme used in Table 2. The methyl groups in *tert*-butyl groups were omitted for the sake of clarity. The ruthenium(III) is coordinated in an octahedral arrangement by the oxygen atoms of three β -diketonate ligands. Complex **3** is obviously identified as a tris(β -diketonato)ruthenium(III) complex with an ene-yne group on the chelate ring, $[\text{Ru}(E-1,4\text{-mBSima})(\text{dpm})_2]$.

[Table 1]

[Table 2]

[Fig. 1]

We consider two structural isomers as a presumable candidate for **4**, one is the *E* form of $\{3\text{-}(2,4\text{-bis}(\text{trimethylsilyl})\text{-}1\text{-butene-}3\text{-ynyl})\text{-}2,4\text{-pentanedionato}\}\text{-Ru}(\text{dpm})_2$ ($[\text{Ru}(E-2,4\text{-mBSima})(\text{dpm})_2]$), another is the *Z* form of $\{3\text{-}(1,4\text{-bis}(\text{trimethylsilyl})\text{-}1\text{-butene-}3\text{-ynyl})\text{-}2,4\text{-pentanedionato}\}\text{-Ru}(\text{dpm})_2$ ($[\text{Ru}(Z-1,4\text{-mBSima})(\text{dpm})_2]$) as shown in Chart 1 together with $[\text{Ru}(E-1,4\text{-mBSima})(\text{dpm})_2]$ (**3**). According to the results of spectroscopic measurements, difference in molecular structure between complexes **3** and **4** is not slight. Compared to complex **3**, complex **4** has higher molecular symmetry (C_2) in solution, indicating the ethene plane in complex **4** would rotate or be fixed to β -diketonato chelate plane with precise vertical. This produces possibility that both of the two structural isomers might be complex **4**, because the ethene plane in $[\text{Ru}(Z-1,4\text{-mBSima})(\text{dpm})_2]$ can be fixed, and the plane in $[\text{Ru}(E-2,4\text{-mBSima})(\text{dpm})_2]$ can rotate. However, from the view point of paramagnetic contact and/or pseudo-contact shift of the ethene proton, difference in configuration of the ethene proton between **3** and **4** is not small: 4.97 ppm for **3** and 44.6 ppm for **4**. If complex **4** is $[\text{Ru}(Z-1,4\text{-mBSima})(\text{dpm})_2]$,

chemical shift of the ethene proton would exhibit almost the same chemical shift for complex **3** due to the same configuration. Similar tendency is found in the IR spectra; difference in the C≡C stretching band frequencies, 2155 cm⁻¹ for **3** and 2117 cm⁻¹ for **4** indicates that neighbor group of the C≡C group in **3** is different from that in **4**. These considerations allow us to envisage [Ru(*E*-2,4-*mBSima*)(dpm)₂] as complex **4**. In fact, insertion reactions sometimes occur to form ene-yne derivatives in course of the reaction of terminal alkynes with aryl halides by using Pd catalyst [8]. If the insertion reactions, Heck-like reactions occur in our system, two ene-yne ruthenium complexes (**3** and **4**) can form as shown in Scheme 2 expressing reaction mechanism[3b]. In the Heck-like reactions the halide ruthenium and Pd catalyst must locate at *cis* position in the intermediates. Complex **4**, therefore, can be assigned as [Ru(*E*-2,4-*mBSima*)(dpm)₂].

[Chart 1]

[Scheme 2]

3.2 Structural characterization of [Ru(*E*-1,4-*mBSima*)(dpm)₂] (**3**)

The dihedral angle between the least-squares chelate plane (1) through the atoms Ru, O(5), C(24), C(25), C(26), O(6) and the least-squares ethene plane (2) through the atoms Si(1), C(28), C(29), C(30) is 91.04(9)°. The ethene plane slightly cants to a vertical plane of the chelate ring plane. The negligible cant of the ethene plane is ascribed to fixation by intraligand steric hindrance between methyl groups on the chelate ring and those in the trimethylsilyl group. In fact, interatomic distances between C(23) and C(33), and between C(27) and C(34) are 3.53(1) and 3.61(1) Å, respectively, which are significantly close to

twice the van der Waals radius of carbon (3.40Å) [9].

DFT calculations were performed for [Ru(*E*-1,4-mBSima)(dpm)₂] (**3**). The DFT optimized geometry of complex **3** reasonably reproduces the features of the experimental structure (Table 2) within ±0.03 Å in bond length and ±4° in bond angle except for one bond angle. The Si(2)-C(31)-C(30) bond angle in experimental structure is 170.5(6)°, on the other hand 177.6° in calculated structure. The DFT optimization overestimates the Si(2)-C(31)-C(30) bond angle by 4 %. Dihedral angle, 91.02° between planes (1) and (2) in the optimized geometry agrees with the angle, 91.04(9)° in experimental structure data, indicating that the canting of the ethene plane is plausible.

[Fig.2]

Interestingly, we can find evidence that the ethene plane is fixed with negligible canting in ¹H NMR spectrum for complex **1** in solution. The ¹H NMR spectrum of **3** in C₆D₆ at ambient temperature exhibited 10 peaks between 5 and -55 ppm with paramagnetic shift, while **4** exhibited only 7 peaks as shown in Figure 2. For example, **3** exhibited two methyne (=CH) signals at -30.8 and at -54.2 ppm, while **4** had only one signal at -42.4 ppm. This indicates that **3** has no symmetry, *i.e.*, the ethene plane is fixed with canting to the chelate plane even in solution. Detail investigation of the fixation is in progress.

4. Conclusion

Two unexpected ruthenium(III) complexes formed in the course of the Sonogashira reactions have been identified as novel ene-yne complexes, **3** and **4** which are structural

isomers by X-ray crystallography, ^1H NMR and IR spectroscopies, mass spectrometry, and electrochemistry. The ene-yne complexes are formed by the Heck-like reactions, i.e., insertion reactions. The insertion reactions prevent the desired ethynyl complex from forming in good yield. The ethene plane in complex **3** is fixed to the β -diketonato chelate plane either in solid state or in solution state at ambient temperature, supported by X-ray structure analysis, DFT calculation, and the ^1H NMR spectrum with no symmetry. These two ene-yne ruthenium complexes would be useful building blocks for bi- or oligonuclear complexes with ene-yne bridge for vertical direction to chelate plane.

5. Acknowledgement

This research was partially supported by a Grant-in-Aid for Scientific Research (No. 15550052) from the Japan Society for the Promotion of Science and a Grant-in-Aid for Scientific Research on Priority Areas “Chemistry of Coordination Space” No. 17036052 from the Ministry of Education, Culture, Sports, Science and Technology of Japan.

6. Supplementary material

CCDC 810227 contains the supplementary crystallographic data for complex **3**. This data can be obtained free of charge from The Cambridge Crystallographic Data Centre via www.ccdc.cam.ac.uk/data_request/cif.

References

- [1] (a) M. A. Fabre, J. Jaud, J. Bonvoisin, *Inorg. Chim. Acta*, 358 (2005) 2384;
(b) M. A. Fabre, J. Bonvoisin, *J. Am. Chem. Soc.* 129 (2007) 1434;
(c) A. Albinati, P. Leoni, L. Marchetti, S. Rizzato, *Angew. Chem. Int. Ed.* 42 (2003) 5990;
(d) H. L. Anderson, *Chem. Commun.* (1999) 2323;
(e) P. N. Taylor, A. P. Wylie, J. Huuskonen, H. L. Anderson, *Angew. Chem. Int. Ed.* 37 (1998) 986;
(f) K. Sugiura, Y. Fujimoto, Y. Sakata, *Chem. Commun.* (2000) 1105;
(g) N. L. Narvor, L. Toupet, C. Lapinte, *J. Am. Chem. Soc.* 117 (1995) 7129;
(h) M. Guillenot, L. Toupet, C. Lapinte, *Organometallics* 17 (1998) 1928;
(i) F. Paul, W. E. Meyer, L. Toupet, H. Jiao, J. A. Gladysz, C. Lapinte, *J. Am. Chem. Soc.* 122 (2000) 9405;
(j) S. Fraysse, C. Coudret, J.-P. Launay, *J. Am. Chem. Soc.* 125 (2003) 5880;
(k) M. I. Bruce, B. G. Ellis, P. J. Low, B. W. Skelton, A. H. White, *Organometallics* 22 (2003) 3184;
(l) M. I. Bruce, K. Costuas, T. Davin, B. G. Ellis, J.-F. Halet, C. Lapinte, P. J. Low, M. E. Smith, B. W. Skelton, L. Toupet, A. H. White, *Organometallics* 24 (2005) 3864;
(m) C. Hartbaum, E. Mauz, G. Roth, K. Weissenbach, H. Fischer, *Organometallics* 18 (1999) 2619;
(n) M. Brady, W. Weng, Y. Zhou, J. W. Seyler, A. J. Amoroso, A. M. Arif, M. Böhme, G. Frenking, J. A. Gladysz, *J. Am. Chem. Soc.* 119 (1997) 775;
(o) N. Gauthier, C. Olivier, S. Rigaut, D. Touchard, T. Roisnel, M. G. Humphrey, F. Paul, *Organometallics* 27 (2008) 1063.
- [2] (a) Y. Kasahara, Y. Hoshino, M. Kajitani, K. Shimizu, and G. P. Satô, *Organometallics*,

- 11 (1992) 1968;
- (b) Y. Hoshino, T. Suzuki, H. Umeda, *Inorg. Chim. Acta* 245 (1996) 87;
- (c) Y. Hoshino, Y. Hagihara, *Inorg. Chim. Acta*, 292 (1999) 64;
- (d) Y. Hoshino, *Platinum Metal. Rev.* 45 (2001) 2;
- (e) Y. Hoshino, S. Higuchi, J. Fiedler, C.-Y. Su, A. Knödler, B. Schwederski, B. Sarkar, H. Hartmann, W. Kaim, *Angew. Chem. Int. Ed.* 42 (2003) 674;
- (f) K. Aoki, H. Kamo, J. Chen, Y. Hoshino, *J. Electroanal. Chem.* 420 (1997) 189.
- [3] (a) K. Sonogashira, *Comprehensive Organic Synthesis*, vol. 3, Pergamon Press, Oxford, 1991, p. 521;
- (b) K. Sonogashira, Y. Tohda, and N. Hagihara, *Tetrahedron Lett.*, (1975) 4467;
- (c) J. Suffert and R. Ziessel, *Tetrahedron Lett.*, 32 (1991) 757;
- (d) R. Ziessel, J. Suffert, and M.-T. Youinou, *J. Org. Chem.*, 61 (1996) 6535.
- [4] S. Munery, J. Jaud, J. Bonvoisin, *Inorg. Chem. Commun.* 11 (2008) 975.
- [5] M. J. Frisch, et al. *Gaussian 03, Revision C.02*; Gaussian Inc.: Wallingford, CT, 2004.
- [6] (a) K. Burke, J. P. Perdew, and Y. Wang, in *Electronic Density Function Theory: Recent Progress and New Direction*, Ed. J. F. Dobson, G. Vignale, and M. P. Das (Plenum, 1998);
- (b) J. P. Perdew, in *Electronic Structure of Solids '91*, Ed. P. Ziesche and H. Eschring (Akademie Verlag, Berlin, 1991);
- (c) J. P. Perdew, J. A. Chevary, S. H. Vosko, K. A. Jackson, M. R. Perderson, D. J. Singh, and C. Fiolhais, *Phys. Rev. B* 46, (1992) 6671;
- (d) J. P. Perdew, J. A. Chevary, S. H. Vosko, K. A. Jackson, M. R. Perderson, D. J. Singh, and C. Fiolhais, *Phys. Rev. B* 48, (1993) 4978;
- (e) J. P. Perdew, K. Burke, and Y. Wang, *Phys. Rev. B* 54 (1996) 16533.
- [7] "TeXsan, Crystal Structure Analysis Package", Molecular Structure Cooperation (1992).
- [8] J. Tsuji, *Palladium Reagents and Catalysts*, John Wiley & Sons, Chichester, 1995,

pp168-188.

[9] A. Bondi, J. Phys. Chem. 68 (1964) 441.

Figure Captions

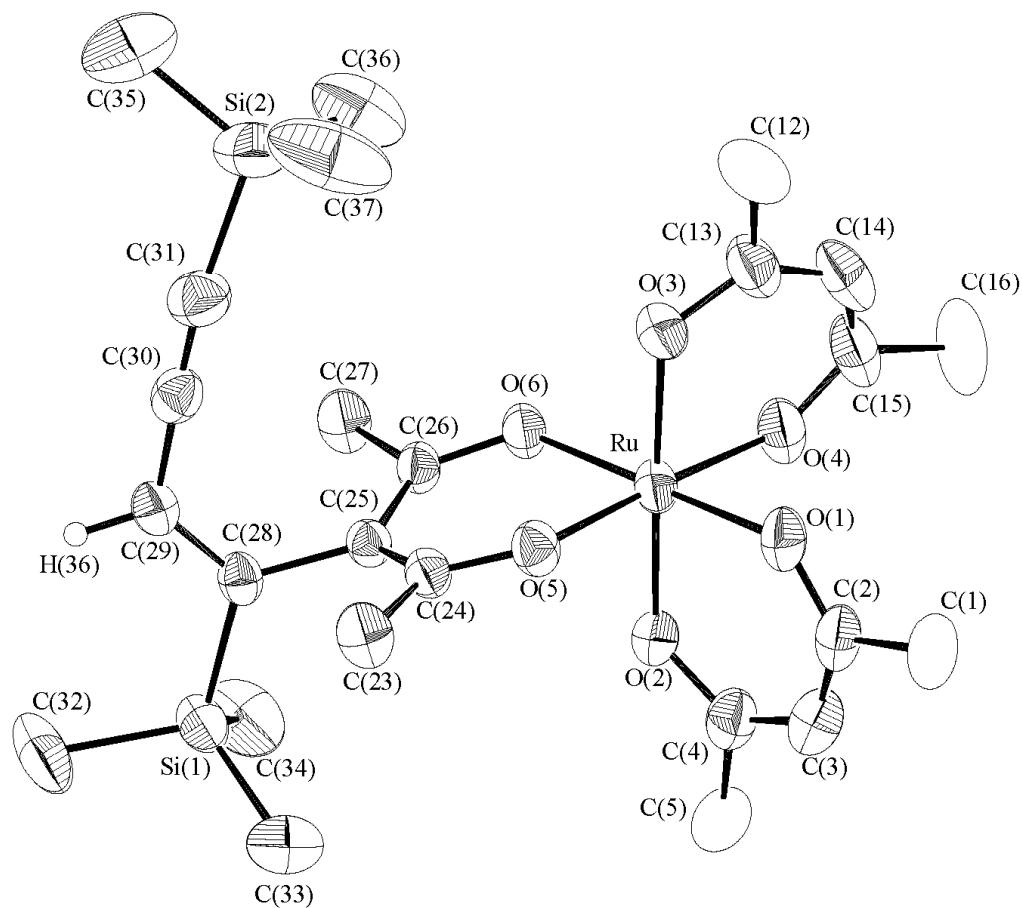


Fig. 1. ORTEP drawing of complex **3** with the numbering scheme of the atoms.

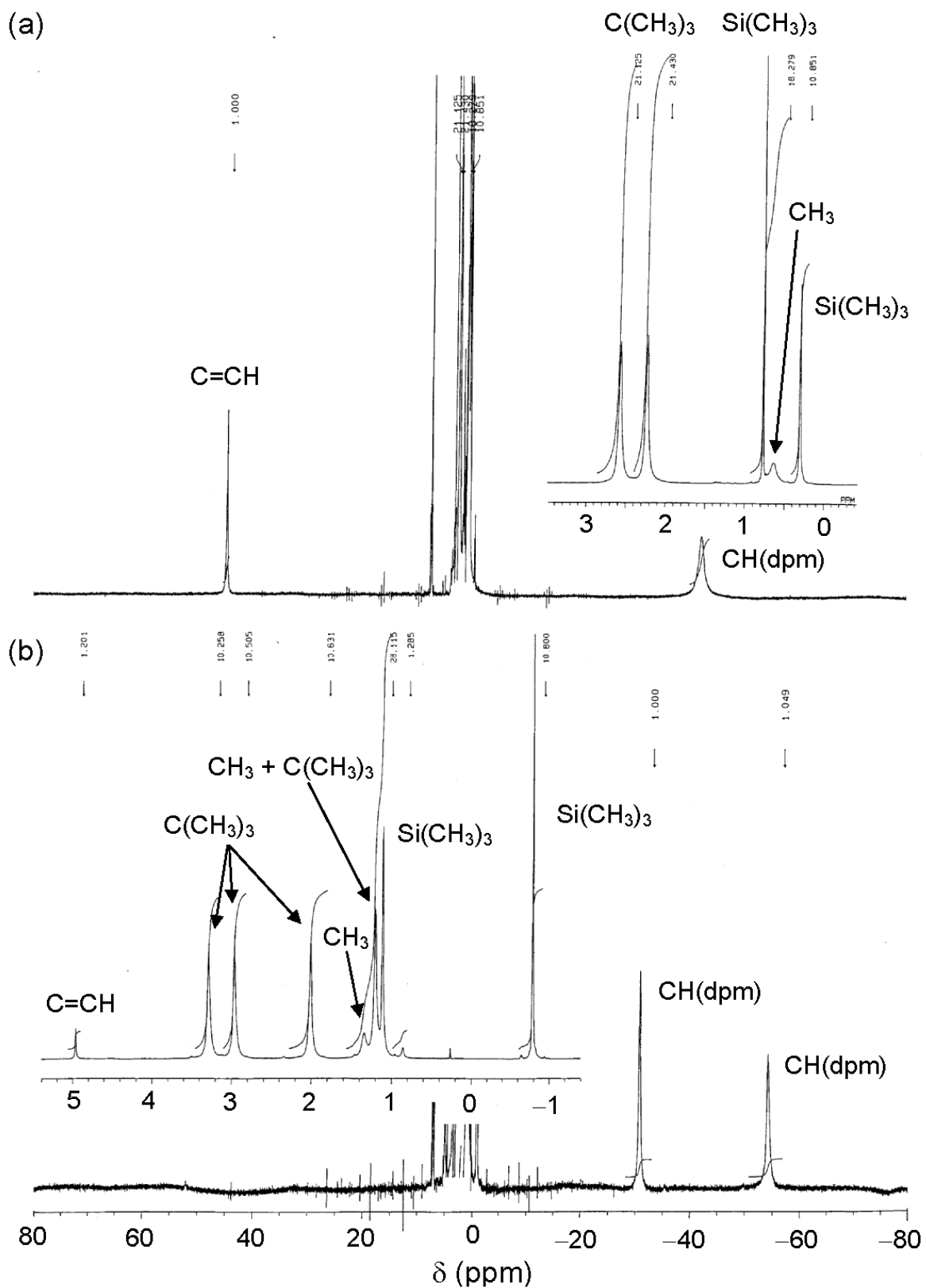


Fig. 2. ^1H NMR spectra of complex **4** ($[\text{Ru}(E-2,4\text{-mBSima})(\text{dpm})_2]$) (a) and complex **3** ($[\text{Ru}(E-1,4\text{-mBSima})(\text{dpm})_2]$) (b) in C_6D_6 at ambient temperature.

Table Captions

Table 1

Summary of the crystal data and structure refinements for [Ru(*E*-1,4-mBSima)(dpm)₂] (**3**).

3	
Empirical formula	C ₃₇ H ₆₃ RuO ₆ Si ₂
Formula weight	761.14
Temperature (K)	288(2)
Crystal system	orthorhombic
Space group	<i>Pbca</i> (#61)
<i>a</i> (Å)	19.958(3)
<i>b</i> (Å)	27.882(4)
<i>c</i> (Å)	16.154(2)
<i>V</i> (Å ³)	8989(2)
<i>Z</i>	8
<i>D</i> _{calc} (g cm ⁻³)	1.125
<i>D</i> _{meas} (g cm ⁻³)	1.128(3)
μ (mm ⁻¹)	0.438
F(000)	3240
Crystal size (mm)	0.26 x 0.14 x 0.14
Max. 2 θ (°)	55.1
No. reflections measured	8526(total)
No. observations [<i>I</i> > 2 σ (<i>I</i>)]	6789
Data/parameters	6789/444
<i>R</i> ^a	0.0773
<i>R</i> _w ^b	0.2178
Goodness-of-fit ^c on	1.214

^a $R = \Sigma(|F_o| - |F_c|) / \Sigma|F_o|$ for $I > 2.0\sigma(I)$ data.

^b $R_w = [\Sigma w(F_o^2 - F_c^2)^2 / \Sigma w F_o^2]^{1/2}$, with $w = 1/\sigma^2(F_o^2)$.

^c Goodness-of-fit = $\{[\Sigma w(|F_o| - |F_c|)^2] / (N_{\text{refl}} - N_{\text{params}})\}^{1/2}$.

Table 2Selected bond distances, angles, and dihedral angle for **3**.

	Exptl ^a	Calcd ^b
Selected bond distances (Å)		
Ru -O(1)	1.997(4)	2.013
Ru-O(2)	1.995(4)	2.025
Ru -O(3)	2.019(4)	2.048
Ru-O(4)	2.008(4)	2.010
Ru -O(5)	1.989(3)	2.015
Ru-O(6)	2.019(3)	2.037
O(5)-C(24)	1.289(6)	1.284
O(6)-C(26)	1.265(5)	1.270
C(24)-C(25)	1.395(6)	1.415
C(25)-C(26)	1.430(6)	1.429
C(25)-C(28)	1.517(6)	1.502
C(23)-C(24)	1.516(7)	1.511
C(26)-C(27)	1.494(7)	1.512
C(28)-C(29)	1.335(7)	1.358
C(29)-C(30)	1.424(7)	1.427
C(30)-C(31)	1.199(8)	1.228
Si(1)-C(28)	1.891(5)	1.912
Si(2)-C(31)	1.839(7)	1.854
Selected angles (°)		
O(1)-Ru-O(2)	93.1(2)	92.9
O(3)-Ru-O(4)	90.7(2)	90.9
O(5)-Ru-O(6)	89.1(1)	88.2
C(24)-C(25)-C(28)	118.0(4)	119.3
C(26)-C(25)-C(28)	118.4(4)	118.5
C(25)-C(28)-C(29)	120.4(4)	122.3
Si(1)-C(28)-C(25)	119.2(3)	119.0
C(28)-C(29)-C(30)	123.4(5)	126.7
C(29)-C(30)-C(31)	175.4(6)	175.5
Si(2)-C(31)-C(30)	170.5(6)	177.6
Dihedral angle (°) between plane(1) and plane(2)		
	91.04(9)°	91.02°
plane(1): Ru, O(5), C(24), C(25), C(26), O(6)		
plane(2): Si(1), C(28), C(29), C(30)		

^a From crystal structure of complex **3**. ^b From DFT optimized geometry of complex **3**.

Chart 1

